Contrib Mineral Petrol (1985) 89:317–329

Contributions to Mineralogy and Petrology

Chemical differences between minerals from mineralizing and barren intrusions from some North American porphyry copper deposits

D.A.F. Hendry[1], **A.R. Chivas**[2], **J.V.P. Long**[3], **and S.J.B. Reed**[3]

[1] Department of Geology and Geophysics, University of Sydney, NSW 2006, Australia
[2] Research School of Earth Sciences, The Australian National University, Canberra, ACT 2600, Australia
[3] Department of Earth Sciences, University of Cambridge, Cambridge, CB2 3EQ, Great Britain

Abstract. Major-element analyses (by electron microprobe) and copper contents (by ion-probe) are reported for primary biotite, amphibole, magnetite, pyroxene, ilmenite, sphene and secondary biotite from intrusive rocks from mineralizing and barren stocks. The districts studied include Christmas, Globe-Miami, Sierrita and Tombstone, in Arizona; Bingham and Alta, Utah; Ely, Nevada; and Brenda, British Columbia.

Amphiboles from barren rocks are relatively iron-rich and display only minor compositional variation. In contrast, amphiboles from mineralizing rocks span the range from magnesio-hornblende to actinolite, commonly even within one grain.

Barren intrusions (type B) that are temporally distinct from mineralizing intrusions, and barren intrusions outside areas of known mineralization have higher Cu contents in their constituent minerals than do mineralizing intrusions.

Barren intrusions (type A) that are deep-level temporal equivalents of Cu-bearing porphyritic rocks are depleted in copper. This suggests that copper is abstracted from not only the apical portions of porphyries but from parts of the deeper parent intrusions.

The Cu contents of biotites (av. 23 ppm) and magnetites (97 ppm) from barren type B intrusions contrast with those from mineralizing intrusions, with biotites containing 7 ppm Cu and magnetites 3 ppm Cu. Primary amphiboles from all intrusive rock types have low copper contents, typically 2 to 5 ppm.

In the continental North American deposits, the amount of copper available by liberation from or non-incorporation into amphibole, biotite and magnetite during magmatic crystallization or the early hydrothermal stage is low, perhaps too low to be the sole source of copper mineralization, unless copper is abstracted from large volumes (~ 100 km^3) of rock. These results contrast with a study of the island-arc porphyry copper at Koloula, Guadalcanal, where it was argued that sufficient copper for mineralization could have been abstracted from relatively small volumes of host rocks that originally contained as much Cu as the contemporaneous barren rock types.

Introduction

We present here the results of ion-probe analyses of copper contents of biotites, amphiboles and magnetites from specific, well documented North American porphyry copper deposits. Our purpose is to document chemical differences between minerals from mineralizing and barren intrusions and to examine processes by which copper is non-incorporated or lost from silicate phases during vapour exsolution. Support for a magmatic source of copper in porphyry copper deposits has, in recent years, gained strength, following the classic studies of Holland (1972). He demonstrated that base metals in granitic magmas can be extracted in sufficient quantity by an exsolved, chloride-rich aqueous phase to form an economic deposit. That high temperature, chloride-rich magmatic fluids are indeed exsolved from mineralizing intrusions is shown by numerous fluid inclusion and stable isotope studies (e.g. Sheppard et al. 1971; Nash and Cunningham 1974; Sheppard and Gustafson 1976).

In a felsic magma system with the presence of a separate vapour phase, those components that are strongly partitioned into the vapour phase are depleted in the silicate melt and probably even more so in crystallizing amphiboles. It appears that compositional differences in amphiboles and biotites depend on the degree of oxidation imposed on the magma by vapour exsolution (Czamanske and Wones 1973; Chivas 1976, 1981 and Mason 1978). These observations are generally in good agreement with the experimental results of Ryabchikov (1963), Kilinc and Burnham (1972), and Hards (1976). Magmatic oxidising trends can, therefore, be equated with mineralizing trends if sufficient Cl is present in the magma and if enough Cu also is present. There may be cases where vapour exsolution occurs but Cl and/or Cu content are insufficient to cause significant mineralization (e.g. Finnmarka; Czamanske and Wones 1973). Further support for non-incorporation or loss of copper from silicate phases during vapour exsolution is found in an earlier study in an island-arc setting at Koloula, Guadalcanal (Chivas 1981; Hendry et al. 1981). We showed that the mafic minerals from barren intrusions at Koloula have higher-than-normal Cu contents indicating that possibly the intrusive complex as a whole was enriched in Cu, but that only in those intrusive phases in which magmatic boiling occurred did fluids abstract this Cu. Thermodynamic calculations and experimental data on Cu partition coefficients between melt and vapour phase are in agreement with such a conclusion (Candela and Holland 1984).

The use of the terms loss or non-incorporation to describe abstraction of Cu from a felsic magma by an exsolving vapour is deliberate as we are uncertain of the exact mechanisms involved. Feiss (1978) proposed, on the basis of ligand field theory, that the partitioning of Cu between

---

Offprint requests to: A.R. Chivas

Table 1. Copper deposits and intrusions examined in this study

Igneous rock or complex	Age	K–Ar age[a] range of complex	References for K–Ar ages	References for most recent geological description
Alta, UT	early Oligocene	34–33	Crittenden et al. 1973	Cranor 1974
Bingham, UT	late Eocene	39.8–36.6	Warnaars 1978	Lanier et al. 1978
Globe-Miami, AZ	Paleocene	63–59	Creasey 1980	Creasey 1980
Sierrita, AZ	Paleocene	69–58	Cooper 1973	West and Aiken 1982
Tombstone, AZ	late Cretaceous/ Paleocene			Gilluly 1956
Christmas, AZ	late Cretaceous	82–63	Koski and Cook 1982	Koski and Cook 1982
Ely, NV	early Cretaceous	112	McDowell and Kulp 1967	Westra 1979, 1982
Brenda, BC	Jurassic	171, 152 (?)	White et al. 1968	Soregaroli 1974 Soregaroli and Whitford 1976

[a] all ages calculated using decay constants recommended by Steiger and Jäger 1977

silicate melt and early-formed crystalline phases may control the availability of Cu during generation of a postmagmatic fluid phase. Implicit in his approach is the assumption that sequestering of Cu in these minerals is permanent. However other processes that may be significant include diffusion and leaching of Cu from phenocrysts by magmatic fluids as well as late alteration processes such as liberation of Cu by sericitization.

Sampling strategy

In this study the mining districts examined include the Christmas, Globe-Miami, Sierrita and Tombstone districts of Arizona, Bingham in Utah, Ely in Nevada, and Brenda in British Columbia. The deposits cover a variety of ages and tectonic settings (Table 1). The intrusions include both biotite+amphibole (e.g. Christmas) and biotite only (e.g. Globe-Miami) rock types. In selecting suitable samples we concentrated on three distinctive lithologies, common to most porphyry systems, namely high-level Cu-bearing porphyries, equigranular stocks associated with such Cu-bearing porphyries, and associated dykes and/or sills. Our sampling strategy is based on the following premises. Creasey (1980) attributes the aphanitic textures of the groundmass in Cu-bearing porphyries to sudden venting of the H_2O-rich magma chamber. Firstly, we presume that as such fluids migrated upwards, streaming through the upper levels of the porphyritic mass (as evidenced by the presence of breccia pipes) mafic minerals growing in this late magmatic/hydrothermal environment might be expected to incorporate some of the Cu from these fluids. Secondly, in continental North America, Cu-bearing porphyries commonly grade both laterally and vertically into much larger volume, equigranular intrusions. For example equigranular rocks at Bingham outcrop over at least 12 km^2, whereas those at Brenda are of batholithic dimension. Westra (1979) describes in detail a possible relationship between equigranular rocks and Cu-bearing porphyries at Ely where a thermally driven convection cell forced initially water-undersaturated silicate melt through a water saturation surface located below an extensively fractured early quartz monzonite porphyry. This caused the magma to release heat and volatiles before it sank back into the magma chamber, finally crystallizing as an equigranular quartz monzonite. In this way a very large volume of magma contributed volatiles and Cu to the hydrothermal system, located within the fractured porphyry. This abstraction of Cu is potentially sufficiently large to produce an ore deposit. For the Koloula island-arc setting, we calculated that for a cylindrical volume of rock of diameter 1.5 km and height 1 km the equivalent of 300,000 tonnes of metallic Cu could be liberated (Hendry et al. 1981). If such a system were to operate in continental North America, in the manner suggested by Westra (1979), we would expect that mafic minerals located in equigranular stocks in the vicinity of Cu-bearing porphyries would have very low Cu contents. To measure the extent of possible Cu-loss throughout the volume of a typical equigranular stock, we sampled that at Bingham over much of its outcrop area. Finally, dykes and sills located within mining districts are unlikely to have undergone such large-scale thermal convection as equigranular stocks, given their dimensions. We anticipated that Cu contents in mafic minerals within dykes and sills would therefore approach background values, i.e. Cu contents indicative of rocks where volatile loss has not occurred. Data for dykes and sills thus provide a possible reference for which data for equigranular stocks and productive porphyries can be compared.

Experimental technique

Ion probe measurements were carried out using the AEI IM-20 instrument in the Department of Earth Sciences, University of Cambridge. The bombarding beam of $^{16}O^-$ ions had a diameter of about 15 μm, with a current of 15 nA. For Cu analysis the ^{63}Cu peak was compared with ^{54}Fe using a mass resolution of 2,000 in order to separate ^{63}Cu from interfering molecular peaks. Each peak was recorded by step-scanning with small increments of magnetic field, the total counting time being 20 minutes per analysed point. A fitting procedure was used to estimate the background under the ^{63}Cu peak contributed by the sloping tail of the adjacent molecular peak. The Cu concentration was calculated from the relative peak intensity, using data for the relative yield of Cu^+ and Fe^+ ions obtained from standards of known composition. Further details of the analytical procedure can be found in an earlier paper (Hendry et al. 1981).

Complete ion-probe analyses (1,120 analyses) are presented in Table 2. Each result (in ppm Cu) is from a single microarea in one or more grains within a single thin section. Sequential analysis of the same microarea by electron- and ion-probe techniques was achieved by recording the location of each area on photomicrographs. Optically detectable inclusions or chloritized domains were avoided. The latter are commonly Cu-rich (up to 1,000 ppm) and thus throw doubt on the accuracy of earlier studies involving mineral separates (e.g. Parry and Nackowski 1963; Al-Hashimi and

Table 2. Copper contents of minerals analysed by ion-probe. All values in ppm, unless otherwise stated

Rock type/unit	Sample no.	Primary biotite	Secondary biotite	Amphibole	Pyroxene	Magnetite	Ilmenite	Chlorite	Sphene or epidote
Christmas Mine area									
Granodiorite Christmas intrusive complex	C-1 (UG-16-7)	2, 3, 3, 3, 3, 3, 4, 6, 7, 15	n.a.	$^1/_2$, $^1/_2$, 1, 1, 1, 1, 1, 1, 1, 1, 1, 1, 1, 1, 2, 3, 3, 5, 6, 8, 180	n.a.	0, $^1/_2$, $^1/_2$, 1, 1, 1	n.a.	n.a.	n.a.
Biotite granodiorite porphyry Christmas intrusive complex	C-2 (AB-77F-73)	2, 5, 7, 8, 9, 10, 12, 15, 16, 17, 22, 25	2, 6, 9, 10, 12, 21, 27, 29	1, 2, 2, 2, 2, 3, 4, 4, 14, 19, 25, 220	n.a.	1, 1, 2, 3, 11	32	17, 23, 54	n.a.
Quartz diorite Christmas intrusive complex	C-3 (D178-1011)	4, 4, 5, 5, 6, 6, 9, 12	3, 6, 7, 8, 8	1, 1, 1, 2, 2, 2, 2, 2, 3, 4, 5, 7, 7, 17, 18, 38	n.a.	$^1/_2$, 1, 2, 4, 12, 104	n.a.	n.a.	n.a.
Biotite granodiorite porphyry Christmas intrusive complex	C-4 (KC-20-73)	30, 68, 76, 82, 100, 160, 180, 270, 380, 765	n.a.	$^1/_2$, 1, 1, 1, 1, 2, 3, 4, 5, 6, 6, 9, 12, 21, 26, 115, 137, 230, 370, 570, 775	n.a.	2, 2, 2, 3, 4, 7, 430, 2530, 2540, 4100	40	510, 650, 730, 770, 980	n.a.
Quartz diorite Christmas intrusive complex	C-5 (KC-12-73)	7, 9, 10, 11, 12, 13	11, 11, 13, 14, 15	5, 7, 9, 9, 20, 27, 35, 78	n.a.	5, 6, 7, 7, 11, 24	n.a.	n.a.	n.a.
Hornblende rhyodacite porphyry (McDonald stock)	C-6 (Mac-1-72)	n.a.	n.a.	$^1/_2$, $^1/_2$, 1, 1, 1, 1, 1, 1, 2, 2, 2, 2, 2, 2, 2, 2, 2, 3, 3, 3, 5, 5, 6	n.a.	8, 29, 49, 60, 82, 92	n.a.	n.a.	n.a.
Hornblende rhyodacite porphyry (McDonald stock)	C-7 (83AB75)	n.a.	n.a.	1, 1, 1, 1, 1, 2, 2, 2, 2, 3, 5, 5, 8	n.a.	85, 207, 450, 475	20, 21, 35	n.a.	c = 11
Hornblende rhyodacite porphyry (Granite Basin pluton)	C-8 (GB-1)	25, 31, 47, 57	n.a.	1, 1, 1, 1, 1, 2, 2, 2, 2, 2, 2, 2, 2, 2, 3, 3, 3, 4, 5, 6, 9	n.a.	6, 42, 84, 160, 270, 740	n.a.	n.a.	n.a.
Hornblende rhyodacite porphyry dyke	C-9 (AB70-73)	n.a.	n.a.	1, 1, 1, 2, 2, 2, 2, 2, 2, 2, 2, 2, 3, 18	n.a.	7, 12, 15, 18, 19, 44	n.a.	n.a.	e = 1, 2
Hornblende andesite porphyry dyke	C-10 (72AB74)	n.a.	n.a.	$^1/_2$, 1, 1, 1, 1, 2, 2, 2, 2, 2, 2, 2, 2, 2, 2, 2, 2, 2, 3, 3, 3, 3, 3, 3, 3, 3, 4, 5, 9	n.a.	6, 13, 14, 22, 22, 24, 27, 27, 30, 42, 53, 62	n.a.	n.a.	n.a.
Hornblende andesite porphyry dyke	C-11 (5AB74)	n.a.	n.a.	$^1/_2$, 1, 2, 4, 4, 4, 5, 5, 5, 5, 7, 8, 9, 10, 10, 13, 14, 17	n.a.	57, 72, 102, 162, 187	48	n.a.	n.a.
Hornblende andesite porphyry dyke	C-12 (53AB75)	n.a.	n.a.	3, 3, 4, 4, 4, 4, 4, 4, 5, 5, 5, 5, 5, 5, 6, 8, 17, 18	n.a.	42, 44, 45, 65, 115, 245	n.a.	n.a.	n.a.
Globe-Miami [Schultze Granite]									
Main phase	GM-1	3, 4, 5, 5, 5, 14, 15, 17, 23	n.a.	n.a.	n.a.	2, 3, 3, 5, 7, 40	n.a.	n.a.	n.a.
Main phase	GM-2	2, 2, 2, 3, 3, 4, 4, 6, 6, 7, 8	n.a.	n.a.	n.a.	30, 37, 45, 61, 62, 65	n.a.	20, 23, 26, 39	n.a.

Table 2 (continued)

Rock type/unit	Sample no.	Primary biotite	Secondary biotite	Amphibole	Pyroxene	Magnetite	Ilmenite	Chlorite	Sphene or epidote
Porphyry phase (Oxhide)	OX	20, 25, 38, 39, 50, 57, 104, 130, 310, 340, 1100	n.a.	n.a.	n.a.	n.a.	5, 5, 21	n.a.	n.a.
Granodiorite (Pinto Valley)	PV-1	24, 40, 63, 96, 114, 140, 160, 200, 300	n.a.	n.a.	n.a.	0.09%, 0.11%, 0.70%	1, 2, 2	n.a.	n.a.
Porphyry phase (Diamond H)	◇ H	5, 8, 9, 10, 10, 11, 11, 11, 13, 23	n.a.	n.a.	n.a.	n.a.	n.a.	10, 17, 23, 24, 36, 43	n.a.
Porphyry phase (Copper Cities)	CC-1	3, 4, 6, 7, 9, 9, 9, 23	n.a.	n.a.	n.a.	90	n.a.	51, 62	n.a.
Porphyry phase (Copper Cities)	CC-2	0, $^1/_2$, $^1/_2$, $^1/_2$, 1, 1, 2, 2, 4, 10	n.a.	n.a.	n.a.	$^1/_2$, 2, 2, 7	2	n.a.	n.a.
Other Arizona samples									
Ruby Star quartz monzonite porphyry (Sierrita)	S-1	2, 2, 3, 3, 4, 4, 7, 13	n.a.	n.a.	n.a.	0, $^1/_2$, $^1/_2$, 1, 1, 3	n.a.	n.a.	n.a.
Schieffelin granodiorite (Tombstone)	TS	4, 5, 8, 9, 13, 13, 30, 48	n.a.	1, 1, 2, 12, 69, 270	n.a.	5, 7, 11, 17, 33, 255	n.a.	36, 65, 69, 100, 110	n.a.
Bingham									
Quartz latite porphyry	BI-1	1, 2, 2, 2, 2, 3, 3, 3, 3, 3, 3, 3, 4, 4, 5, 5, 7	7, 8, 11, 18, 18, 41	n.a.	n.a.	3, 3, 5	15	n.a.	$s=17$, 18, 20
Latite porphyry	BI-3	18, 18, 34, 42	35, 56, 70, 95, 105, 116, 122	n.a.	n.a.	n.a.	n.a.	n.a.	n.a.
Quartz monzonite porphyry	BI-2	11, 12, 16, 21	8, 9, 15, 15, 15, 19, 20, 21	n.a.	n.a.	n.a.	n.a.	n.a.	n.a.
Ohio Copper dyke	BI-8	2, 3, 5, 6, 6, 7, 9, 10, 10, 13, 14, 15, 22	n.a.	n.a.	1, 5, 5, 7, 18, 18	2, 6, 9, 11, 19, 20	n.a.	n.a.	n.a.
Quartz monzonite	BI-4	5, 5, 8, 8, 9, 10, 10, 13, 13, 17, 19, 20	4, 8, 12, 20, 50, 60, 80, 200	n.a.	n.a.		n.a.	n.a.	n.a.
Quartz monzonite	BI-5	0, 0, $^1/_2$, $^1/_2$, $^1/_2$, $^1/_2$, $^1/_2$, $^1/_2$, 1, 1, 1, 2, 2, 2, 2, 3, 6, 8	n.a.	n.a.	n.a.	n.a.	n.a.	n.a.	n.a.
Monzonite	BI-6	2, 4, 5, 5, 6, 6, 7, 11, 11, 12, 13, 14	n.a.	$^1/_2$, 1, 1, 3, 3, 3, 3, 3, 4, 4, 6, 6, 6, 9, 15	n.a.	6, 8, 8, 8, 19, 22	n.a.	18	n.a.
Monzonite	BI-9	0, 2, 2, 2, 3, 3, 3, 4, 6, 6, 22	n.a.	n.a.	0, $^1/_2$, $^1/_2$, 1, 1, 1, 1, 1, 1, 2, 2, 2	1, 1, 1, 1, 9	n.a.	n.a.	n.a.
Monzonite	BI-10	2, 3, 4, 4, 4, 5, 5, 9, 20	n.a.	n.a.	$^1/_2$, $^1/_2$, $^1/_2$, 1, 1, 1, 1, 1, 2, 3, 3, 3, 3, 3	2, 2, 2, 3, 4, 15	n.a.	n.a.	n.a.
Last Chance stock (monzonite)	BI-11	2, 4, 5, 6, 6, 6, 7, 7	n.a.	1, 2, 2, 3	1, 1, 1, 3, 3, 7	1, 2, 4, 10, 66	n.a.	n.a.	n.a.

Table 2 (continued)

Rock type/unit	Sample no.	Primary biotite	Secondary biotite	Amphibole	Pyroxene	Magnetite	Ilmenite	Chlorite	Sphene or epidote
Last Chance stock (monzonite)	BI-12	4, 4, 5, 6, 9, 9, 13, 14, 16	n.a.	n.a.	4, 30	6, 9, 11, 11, 16	n.a.	n.a.	n.a.
Last Chance stock (monzonite)	BI-13	2, 3, 4, 7, 14, 17	n.a.	6, 9, 27, 30, 33, 35, 42, 42, 45, 57	n.a.	3, 3, 3, 5, 7, 18	n.a.	n.a.	n.a.
Alta Stock									
Porphyritic phase	AS-IS	1, 2, 2, 3, 3, 4, 4, 21	n.a.	1, 1, 2, 2, 2, 3, 5, 6, 53	n.a.	1, 2, 4, 7, 14, 15, 0.25%, 1.5%	n.a.	38, 43, 90	n.a.
Equigranular phase	AS-7A-1	2, 2, 2, 2, 2, 3, 8	n.a.	1, 1, 2, 2, 3, 3, 5, 6, 7	n.a.	1, 1, 1, 2, 2, 2, 3, 4, 382	n.a.	8, 9, 20, 27	s = 5, 16, 26, 28
Equigranular phase	AS-7A-2	11, 11, 13, 20, 44	n.a.	1, 1, 1, 1, 1, 2, 4, 5	1, 1, 2, 28, 295	$^1/_2$, 2, 9, 17, 85, 110, 1.05%	n.a.	240, 260, 290	n.a.
Brenda									
Quartz diorite	B-1	0, $^1/_2$, 1, 1, 1, 1	n.a.	0, $^1/_2$, $^1/_2$, $^1/_2$, 2, 2, 47, 75	n.a.	0, 2, 2, 4, 11	n.a.	n.a.	n.a.
Granodiorite	B-2	2, 2, 3, 3, 4, 15, 17, 17	n.a.	0, 1, 1, 1, 1, 1, 1, 2, 4, 4, 4, 7	n.a.	0, 2, 4, 5, 5, 11	n.a.	n.a.	s = 9, 10, 10, 19
Granodiorite	B-3	$^1/_2$, 1, 1, 2, 2, 13, 56	n.a.	0, 1, 1, 1, 1, 1, 2, 2, 2, 3, 6, 32, 110	n.a.	1, 2, 3, 5, 6	n.a.	n.a.	s = 2, 3, 5
Aplite dyke	B-6	2, 2, 4, 4, 10	n.a.	n.a.	n.a.	9, 12, 38, 55, 60	n.a.	n.a.	n.a.
Ely									
Late-stage hornblende porphyry	E-2	7, 9, 14, 18	n.a.	0, 0, 0, $^1/_2$, 1, 4	n.a.	2, 2, 3, 6, 19	n.a.	n.a.	s = $^1/_2$, 2, 3, 13
Late-stage hornblende porphyry	E-4	2, 3, 3, 5	n.a.	1, 1, 1, 1, 1, 1, 1, 1, 1, 2, 2, 2, 2, 2, 2, 4, 190	n.a.	3, 6, 11, 16, 16, 29	n.a.	n.a.	s = 13, 15, 15, 19
Weary *Flat* quartz monzonite	E-1	n.a.	n.a.	$^1/_2$, 1, 1, 1, 1, 1, 2, 3, 3, 4, 4, 6	n.a.	$^1/_2$, 1, 2, 3, 9	n.a.	n.a.	s = 3, 4, 5, 10, 10, 16, 17
Lane Valley sill	E-8	n.a.	n.a.	1, 1, 1, 1, 1, 1, 1, 1, 1, 2, 2, 3, 5, 15, 19	n.a.	3, 4, 9, 10, 12, 13	n.a.	n.a.	s = 12, 14, 15, 18, 20, 22
Lane Valley sill	E-9	2, 6, 6, 7, 43	n.a.	$^1/_2$, $^1/_2$, $^1/_2$, 1, 1, 1, 1, 1, 1, 1, 2, 2, 2, 2, 2, 2, 3, 4, 6, 9, 10, 20, 33	n.a.	7, 12, 15, 90, 230, 0.12%	n.a.	n.a.	s = 2, 4, 8, 9, 11, 13
Ore sample from quartz monzonite porphyry	3E	n.a.	5, 6, 12, 35	n.a.	n.a.	n.a.	n.a.	n.a.	n.a.
Ore sample from quartz monzonite porphyry	3E-666 (56642)	n.a.	1, 1, 2, 5, 7, 82	n.a.	n.a.	n.a.	n.a.	n.a.	n.a.

e = epidote; s = sphene; n.a. = not analysed

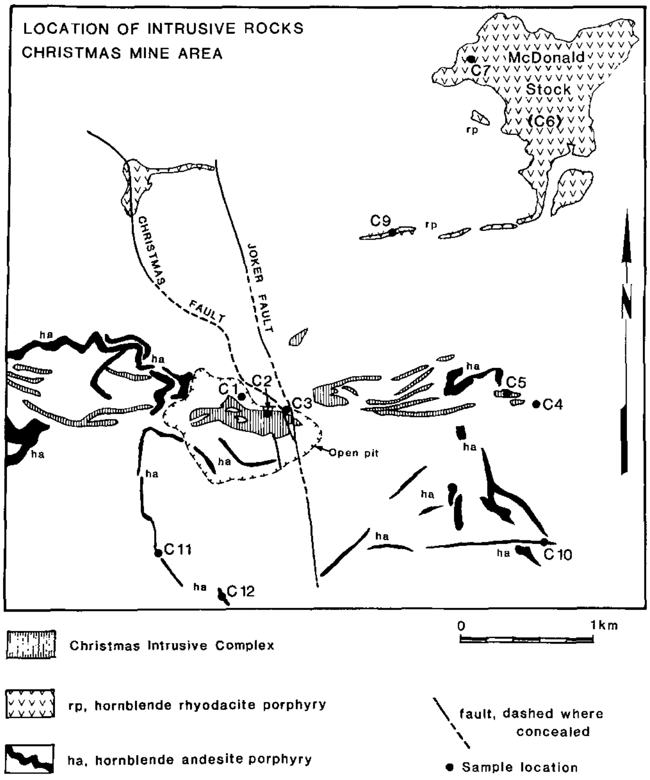

Fig. 1. Geological map after Koski and Cook (1982) and location of samples, Christmas, Arizona. The precise location of sample C6 within the McDonald stock is unknown. Sample C8 derives from the Granite Basin pluton (9 km × 2 km outcrop area) which is 6 km northeast of the McDonald stock

Brownlow 1970; Lovering 1969; Graybeal 1973; Kesler et al. 1975; Olade 1979).

Amphiboles

Chemical differences between amphiboles are best illustrated in samples from the Christmas mine area, Arizona. The locations of analysed samples are shown in Fig. 1 and geological relationships are described in detail by Koski and Cook (1982). A suite of hornblende andesite porphyry dykes (76 to 81 Ma) and intrusive stocks and dykes of hornblende rhyodacite porphyry (68 to 70 Ma) preceded intrusion of the Christmas intrusive complex (61 to 63 Ma), that hosts the ore deposit. Major-element analyses of amphiboles from these three intrusive suites are plotted in Fig. 2. Amphiboles from the hornblende rhyodacite porphyry and hornblende andesite porphyry dykes are relatively Fe-rich and show only limited compositional variation even though some samples are spaced kilometres apart. In contrast, rocks of the Christmas intrusive complex cover the field of magnesio-hornblende through to actinolite, even within one grain in many cases. This zoning mostly takes the form of patchy compositional domains similar to those reported for amphiboles from the granodiorite at Finnmarka (Czamanske and Wones 1973) and at Koloula (Chivas 1981). There are no recognizable regularities in domain distribution such as rims or cores, nor are compositional variations related to cracks or cleavages, with the exception of sample C4. Here individual grains are partially replaced along grain boundaries and cleavage directions by a later generation of actinolite.

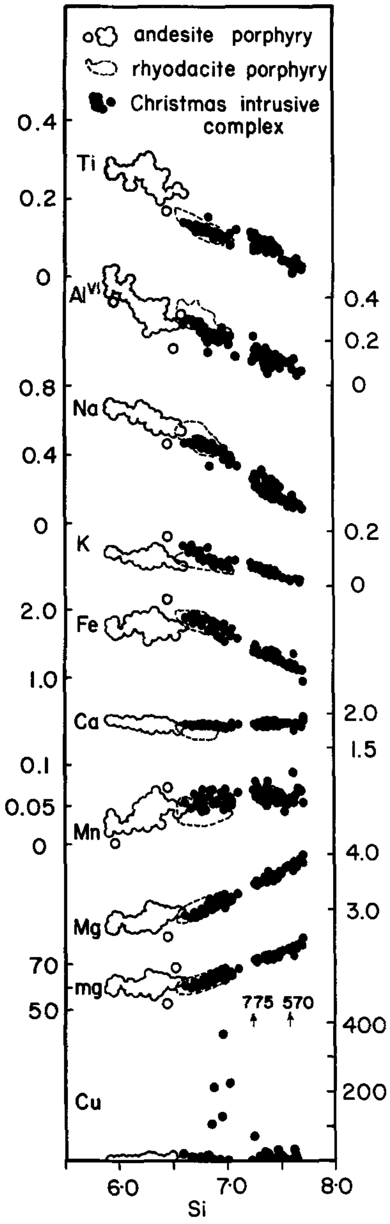

Fig. 2. Elemental variations of amphibole domains with Si content (in atoms per 23 oxygens) from Christmas. Copper content is in ppm. mg = 100 Mg/(Mg + ΣFe). 107 analyses from hornblende andesite dykes, 123 analyses from rhyodacite porphyry stocks and dykes, 106 analyses from the Christmas intrusive complex

Fig. 2 shows elemental variations plotted against silicon content per half-unit cell in Christmas amphiboles. With an increase in Si content there is an increase in Mg and Mn contents, with regular decreases in Fe, Ti, Al^{vi}, Na and K content for Christmas intrusive complex amphiboles. The distribution of Cl in amphiboles of the Christmas intrusive complex is very variable, although trends of Cl versus Si in the unit half-cell are not as clearcut. However, Si-enriched amphibole domains (Si > 7.3) tend to have lower Cl-contents (average 0.055 wt.% Cl) than Si-depleted counterparts (average 0.08 wt.% Cl). Relatively poor detection limits for Cl on the electron probe (0.05 wt.% Cl) may partially obscure this relationship.

Similar trends have been observed in other mining districts. At Ely late-stage hornblende porphyries and the Lane

Valley sill were intruded after ore deposition (McDowell and Kulp 1967). Amphiboles in these barren intrusions show only limited compositional variation, are relatively Fe-rich and Si-depleted (~ 6.35 Si atoms per 23.0). In contrast, amphiboles in the Weary Flat quartz monzonite are markedly more Si- and Mg-rich ($Si > 6.8$). At Ely, the Weary Flat quartz monzonite was probably the source of volatiles and base metals to the hydrothermal system (Westra 1979). The Brenda mine (Soregaroli and Whitford 1976), 225 km east-northeast of Vancouver, is located in the Brenda stock, a composite, zoned quartz diorite to granodiorite body. Amphiboles in both major units of this stock vary in composition from magnesio-hornblende to actinolitic-hornblende. Cl and Ti contents of these amphiboles decrease with increasing Mg and Si, as described for the Christmas intrusive complex. At the Alta stock, located about 40 km southeast of Salt Lake City, minor mineralization is related to porphyritic phases and to adjacent skarns. Amphiboles within the intrusion are zoned and Mg- and Si-rich domains are common.

Two other occurrences of late magmatic/hydrothermal amphibole are noted, that are similar to the late-stage actinolites in sample C4 of the Christmas intrusive complex. At Bingham, hydrothermal amphibole formed both by alteration of pyroxene and as a vein-filling mineral. Compositionally, they are all actinolites ranging from 7.36 to 7.76 Si ions per 23.0. Th second occurrence is from the barren Schieffelin granodiorite, 1.0 km west of Tombstone, Arizona. Hornblendes plot in two separate compositional fields of similar Fe-content, but differing Si content. Most contain between 7.1 and 7.3 Si ions per 23.0, the remainder are more siliceous (Si ~ 7.6) and associated with chlorite.

In summary, amphiboles from dykes, sills and non-mineralized stocks are more Fe-rich and Si-poor than mineralized intrusions, and amphiboles in individual barren intrusions show only limited compositional variation. Amphiboles in Cu-bearing porphyries and equigranular stocks are marked by patchy compositional domains, ranging from magnesio-hornblende through to actinolite, even within single grains. The trend is of increasing Si-content correlated with decreasing Fe, Ti, Al^{vi}, Na, K and Cl contents.

The copper contents of magnetities, amphiboles and biotites from the Christmas area are shown in Fig. 3. Amphiboles in the barren hornblende andesite porphyry dykes and hornblende rhyodacite porphyry have uniformly low Cu-contents, averaging 4.6 ppm and 2.6 ppm respectively. However Figure 3 B shows that there are two different populations of Cu-contents for amphiboles in the Christmas intrusive complex. The higher contents are in the late magmatic/hydrothermal amphiboles (as indicated by other features described above) and the low ones are in magmatic amphiboles. The siliceous nature of Cu-rich amphibole domains is confirmed in Fig. 2 in the plot of Si versus Cu. If Cu-contents of late magmatic/hydrothermal amphiboles are excluded, the remainder in the Christmas intrusive complex average 3.7 ppm, indicating that in the Christmas mine area magmatic amphiboles in both barren and Cu-bearing intrusions have uniformly low Cu-contents.

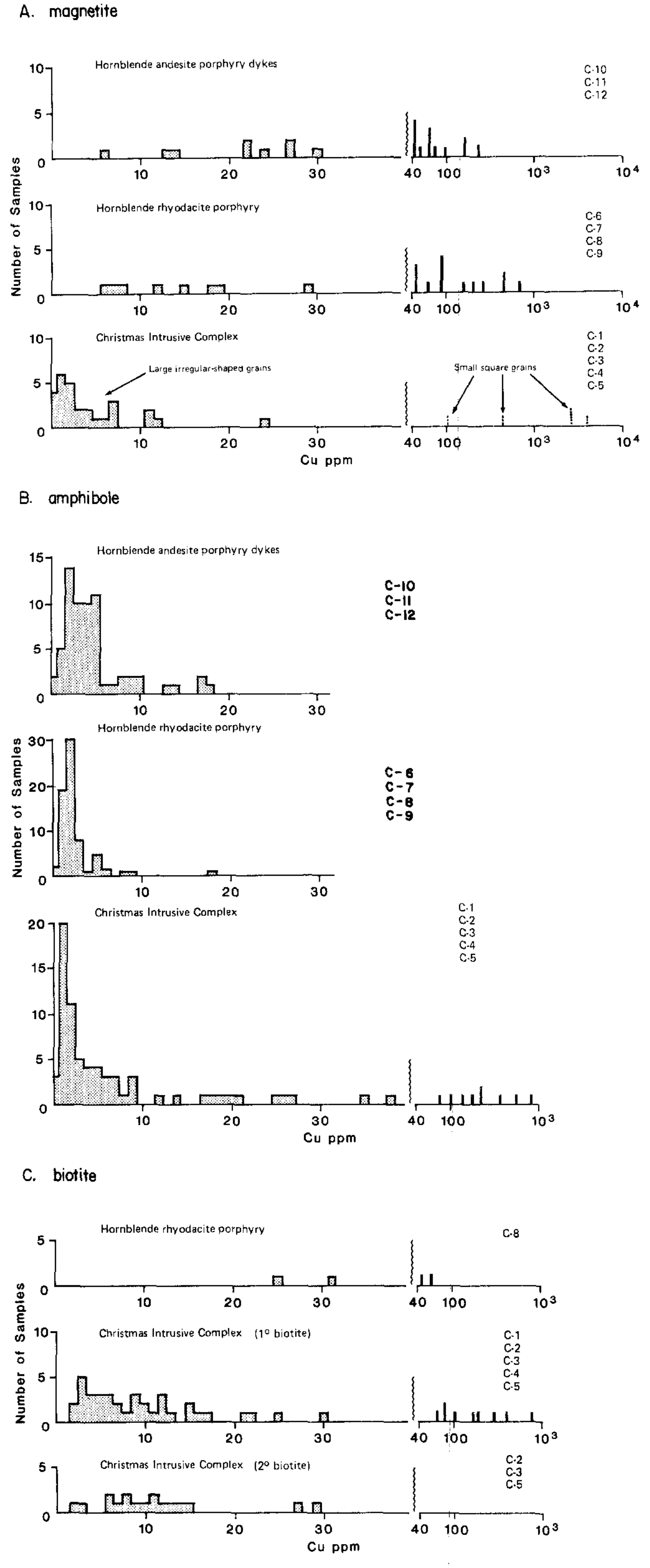

Fig. 3. Copper contents of magnetites, amphiboles and biotites (1° = primary, 2° = secondary) from the Christmas area

Two different populations of Cu-contents are present in other amphibole suites. Data for Ely and Brenda are illustrated graphically in Figs. 4 and 5 respectively. Most amphiboles in all rock types have very low Cu contents, although sporadic high values also occur. Similarly, amphiboles in the Alta stock, listed in Table 2, are all, with one exception, Cu-poor (average 2.7 ppm). We are not sure if these Cu-rich domains are magmatic or reflect later magmatic/hydrothermal events, as supporting textural evidence is lacking. However, Cu-rich amphibole domains at Bingham and in the barren Schieffelin granodiorite are

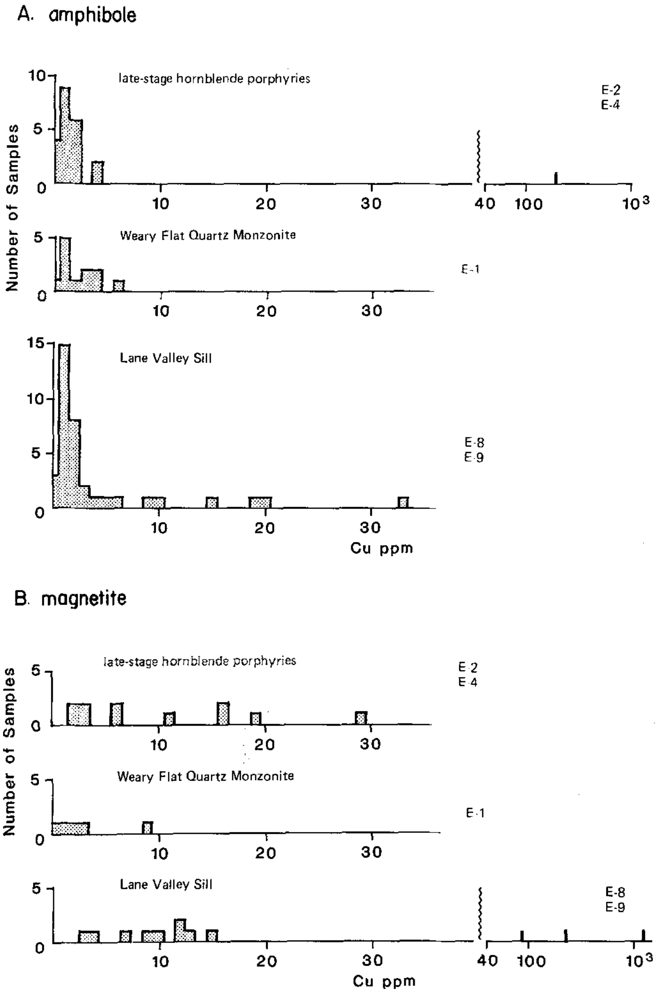

Fig. 4. Copper contents of amphiboles and magnetites from the Ely mine area

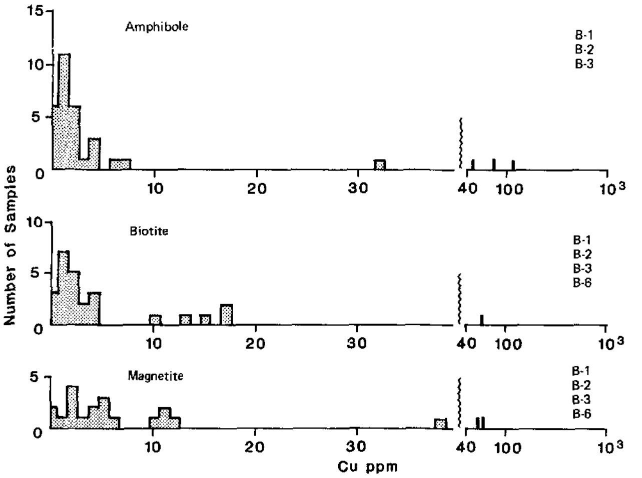

Fig. 5. Copper contents of amphiboles, biotites, and magnetites from the Brenda mine area

clearly late magmatic/hydrothermal features. At Bingham, hydrothermal actinolite formed by alteration of pyroxene has a low Cu-content (average 4.5 ppm) in sample BI-6, a value consistent with low Cu-contents of igneous pyroxenes at Bingham (Table 2). However, more siliceous and Mg-rich actinolites, associated with hydrothermal veins in sample BI-13 also contain markedly more Cu (average 33 ppm). In the Schieffelin granodiorite the low Si-domains are relatively Cu poor (4.0 ppm average). The second more siliceous group is Cu-rich (169 ppm).

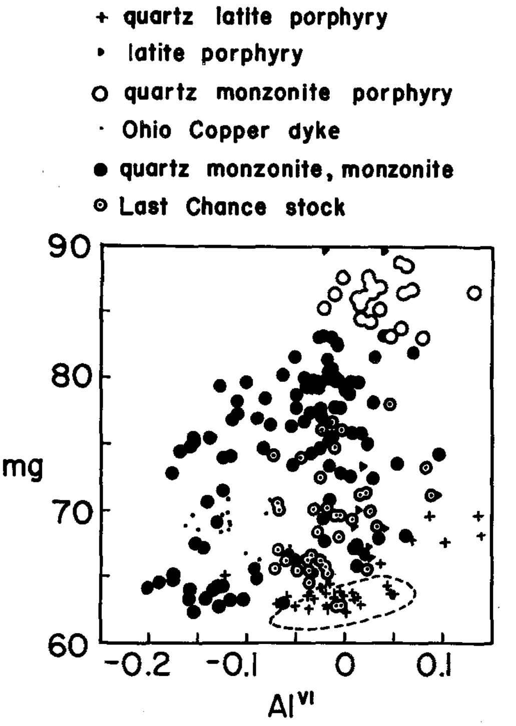

Fig. 6. 100 $Mg/(Mg+\Sigma Fe)$ vs Al^{VI} diagram for biotites from Bingham, Utah. Dashed field encloses 55 biotite analyses from the Christmas intrusive complex. Those analyses that have insufficient $Si+Al$ to form 8 atoms (per 22 oxygens) are depicted as having negative Al^{VI}

In summary, the majority of magmatic amphiboles in the continental North American porphyry copper districts studied contain very little Cu (<5 ppm) in both barren and Cu-bearing intrusions. Actinolites of late magmatic/hydrothermal origin contain appreciably more Cu and values in excess of 500 ppm are recorded (Table 2).

Biotite

In Cu-bearing intrusions at Christmas, Bingham, and Ely, two textural types of biotite occur. The first forms large phenocrysts and is apparently magmatic. Secondary biotite is readily distinguishable from magmatic biotite by its occurrence as small grains, commonly as clumps, and as pseudomorphs associated with sulfides that have replaced primary silicates. Previous studies (e.g. Moore and Czamanske 1973) have noted a greater magnesium content for secondary biotite compared to that of magmatic biotite, but this is not always so. We note that in the Christmas area all primary and secondary biotites plot in a restricted compositional field (Fig. 6). At Bingham, primary and secondary biotites are compositionally similar in some samples (BI-1, BI-2, and BI-5), but distinctly different in others (BI-3 and BI-4). Where compositional differences occur, secondary biotites are invariably richer in magnesium; in sample BI-3 primary biotites have $X_{Mg}=0.70$ and secondary biotites $X_{Mg}=0.92$. Secondary biotites at Ely are also more magnesium-rich than their primary counterparts.

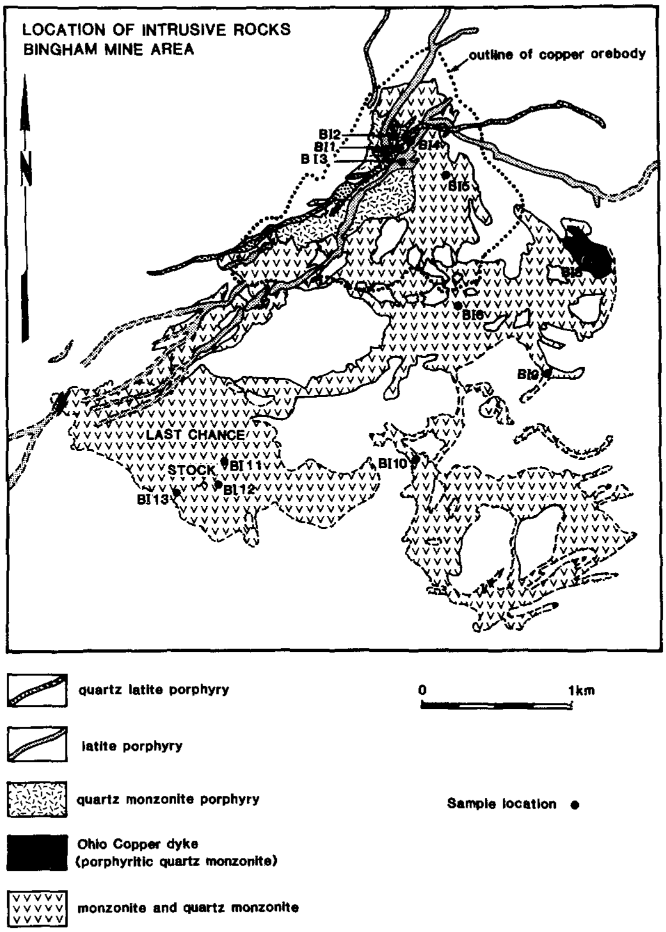

Fig. 7. Geological map (after plate 1, Bray and Wilson 1975) and location of samples, Bingham mining district, Utah

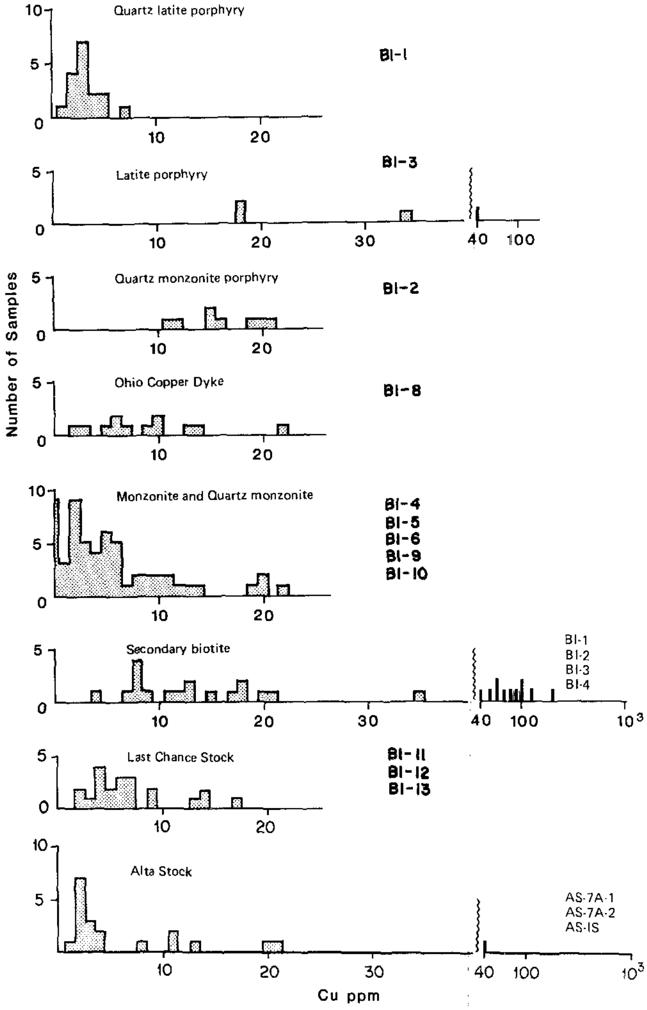

Fig. 8. Copper contents of biotites from rock types from Bingham

Individual primary biotite grains show some compositional variation although it is far less marked than that displayed by amphiboles. The compositions of biotites from six different intrusions at Bingham are plotted in Figure 6, together with Christmas biotites for comparison. The high Mg-content of all magmatic biotites at Bingham is readily apparent with the most Mg-rich biotites present in a sample (BI-2) of quartz monzonite porphyry, the igneous unit spatially associated with hydrothermal alteration and mineralization. At Bingham our eight samples of monzonite and quartz monzonite were collected from within the outline of the copper orebody to 2 km away (Fig. 7). There is no correlation between X_{Mg} of these pre-mineralization biotites and distance from the ore body, suggesting minimal post magmatic, hydrothermal Mg enrichment. Similar results are recorded in the Globe-Miami district for biotites in the composite Schultze Granite. Here, three distinct igneous phases are recognized (Creasey 1980) and of these the larger main phase (unmineralized porphyritic quartz monzonite) and smaller mineralized porphyry phases have been investigated. Biotites in the main phase have average X_{mg} values of 0.55, similar to Cu-bearing porphyries at Pinto valley (X_{mg} 0.56), Diamond H (X_{mg} 0.56) and one sample from Copper Cities porphyry (X_{mg} 0.57). The other sample from Copper Cities porphyry has a slightly higher X_{mg} value of 0.63, as does the sample from the Oxhide porphyry (X_{mg} 0.61).

The Cu contents of magmatic biotites in Cu-bearing porphyries are commonly bimodally distributed. In the Christmas intrusive complex all analysed magmatic biotites, with the exception of those in sample C4, have Cu-contents <30 ppm. Values greater than this (Fig. 3C) come from sample C4, which also contains anomalously Cu-rich amphiboles and magnetites (see below). The Cu-rich biotite domains have similar X_{mg} values to the remainder, in contrast to the distinctive major-element compositions of anomalous Cu-rich amphiboles and magnetites. In the Globe-Miami district, bimodal Cu distributions for biotites in some of the Cu-bearing porphyries can be seen in Table 2; here too Cu-rich magnetites are commonly present. The presence of Cu-rich biotite domains in samples containing secondary Cu-rich amphiboles and magnetites suggests that crystallisation of texturally primary biotite continued into the late magmatic/early hydrothermal stage in some Cu-bearing porphyries.

The Cu contents of magmatic biotites in equigranular stocks, barren porphyries, dykes and sills are all, with one exception, very low. The data for Bingham are illustrated in Fig. 8. Samples BI-11, BI-12 and BI-13, all lying within the Last Chance stock (Fig. 7), differ little from pre-mineralization monzonite and quartz monzonite samples located closer to the ore body. Biotites in the Alta stock, east of Bingham, are also Cu-poor (average 8.0 ppm). The Cu contents of magmatic biotites at Brenda (Fig. 5), for the main phase of the Shultze Granite, for the Ruby Star quartz monzonite porphyry at Sierrita, and Schieffelin granodiorite at Tombstone are all very low (Table 2). The exception is one sample from the Cu-barren Granite Basin pluton (Sample C8, Fig. 3c) that has an average Cu content of 40 ppm.

Secondary biotites have variable Cu-contents. Those in the Christmas intrusive complex average only 11 ppm Cu. At Bingham, secondary biotite is commonly more Cu-rich than magmatic biotite, as shown in Fig. 8, but only in samples in which primary and secondary biotites are compositionally distinct (Samples BI-3 and BI-4, Table 2).

In summary, magmatic biotites show only limited intragrain compositional variation. Our data confirm conclusions of Moore and Czamanske (1973) that, at Bingham, the most Mg-rich biotites are found in the mineralizing porphyry, but this is not so at Christmas and Globe-Miami. The majority of magmatic biotites are Cu-poor, with the exception of some in productive porphyries. These samples also contain Cu-rich secondary actinolite and/or magnetite and a similar origin is likely for the biotites. Two types of hydrothermal biotite are noted. The first, although texturally different from primary magmatic biotite with which it is associated, has similar X_{mg} values to that of magmatic biotite and is Cu-poor. The second, is compositionally distinct with higher X_{mg} values than associated magmatic biotite and is Cu-rich.

Magnetites

In the Christmas area two types of magnetite occur, based on textural and chemical criteria. In hornblende andesite and hornblende rhyodacite porphyries, primary titaniferous igneous magnetite is a common accessory phase, typically occurring as relatively large (1 mm) irregularly-shaped grains. Similarly shaped grains occur in the Christmas intrusive complex, but they are generally Ti-poor. Some of these rocks, e.g. sample C4, contain a second generation of magnetite that occurs as small euhedral grains and is essentially devoid of Ti. This trend of decreasing Ti content of magnetite parallels that already described for amphiboles (Fig. 2). We suggest that this second generation (= secondary) magnetite is late magmatic/hydrothermal in origin, post-dating larger, irregularly shaped magmatic grains at Christmas.

The Cu contents of magnetites from the Christmas intrusive complex are shown in Fig. 3A. Secondary magnetite has a higher copper content than the irregularly-shaped, magmatic magnetites. The Cu contents of magnetites in Cu-bearing porphyries at Pinto Valley and Alta stock are also bimodally distributed (Table 2). If data for texturally secondary magnetites are excluded, primary magnetites in Cu-bearing porphyries and associated equigranular stocks are generally very low. The average Cu-content of magmatic magnetite in the Christmas intrusive complex is 4 ppm. At Bingham, primary magnetite is not observed in samples of mineralized quartz monzonite and latite porphyry. The Cu contents of magnetite in pre-mineralization monzonite and quartz monzonite (8.7 ppm) and Ohio Copper dyke (11.2 ppm) are low as are those in post-mineralization quartz latite porphyry (3.7 ppm). At Ely, magnetite from the Weary Flat quartz monzonite averages 3.1 ppm Cu. In the Globe-Miami district the average is 2.7 ppm for the Copper Cities porphyry (sample CC2) and 10.1 ppm for Ti-poor magnetite in the main phase of the Schultze Granite (sample GM1). Magnetites in the Ruby Star quartz monzonite porphyry at Sierrita (S1) average 1 ppm Cu. The exceptions are titaniferous magnetites in the main phase of the Schultze Granite (GM2) averaging 50 ppm Cu and titaniferous magnetites in a sample of Schieffelin granodiorite (TS) containing sporadic high values (maximum 255 ppm, average 55 ppm). We suggest these latter two samples containing titaniferous magnetities are anomalous and have affinities with magnetites discussed below.

Titaniferous magnetites in hornblende andesite porphyry dykes and hornblende rhyodacite porphyry in the Christmas mine area (Fig. 1) contain average Cu contents of 64 ppm and 134 ppm respectively. These averages are markedly higher than Ti-poor magmatic magnetites in the Christmas productive porphyry (4 ppm). At Ely, average Cu contents of magmatic magnetites (Figure 4) are also higher in the two late-stage barren rock types, particularly for the Lane Valley sill (average 134 ppm Cu), in comparison with the Weary Flat quartz monzonite (average 3.1 ppm Cu).

Other minerals

In many Cu-bearing porphyry samples chlorite has replaced magmatic biotite along grain and cleavage boundaries. In the Christmas intrusive complex, chlorite occurs with either secondary biotite or with secondary magnetite and actinolite. Chlorites in apparent equilibrium with secondary biotite (e.g. sample C2) are, like biotite, Cu-deficient (31 ppm). Those with Cu-rich, secondary magnetite and actinolite (sample C4) are also Cu-rich (average 728 ppm).

Table 2 shows data from sphene (which contains on average 12 ppm Cu), ilmenite (18 ppm Cu), and epidote (5 ppm Cu), for which significant variations in Cu-content were not noted.

Discussion and conclusions

From temporal and field relations alone, we distinguish two categories of barren intrusions, which we refer to as types A and B. Type A barren intrusions are deep-level temporal equivalents of Cu-bearing porphyritic rocks. These barren intrusions are commonly described as equigranular stocks and may have gradational contacts with Cu-bearing porphyries. Examples from this study are the main phase of the Schultze Granite from the Globe-Miami district, Weary Flat quartz monzonite from Ely and the Last Chance stock at Bingham.

Type B barren intrusions occur outside known mining districts or are significantly older or younger than Cu-bearing intrusions in areas of known mineralization. Examples include the Schieffelin granodiorite at Tombstone, which is remote from known Cu-mineralization. In the Christmas area, the hornblende andesite porphyry dykes are 9 to 14 Ma older than the mineralizing event. Similarly, the Granite Basin pluton, McDonald stock and other dykes of hornblende rhyodacite porphyry are 7 Ma years older than the Christmas intrusive complex. At Ely, the Lane Valley sill is post mineralization.

Using this subdivision of intrusions that are either Cu-bearing, barren type A or barren type B (Table 3), it is apparent that barren type B (isolated or temporally unrelated intrusions) have magmatic minerals with higher Cu contents than those intrusions from the other categories. In contrast

Table 3. Summary of copper contents of magmatic biotites, amphiboles and magnetites from mineralizing, barren type A and barren type B intrusions from some North American porphyry copper districts. The data from Koloula, Guadalcanal are from Hendry et al. 1981

	Mineralizing			Barren type A			Barren type B		
	biotite	amph.	magnetite	biotite	amph.	magnetite	biotite	amph.	magnetite
Christmas									
Hornblende andesite porphyry dykes								4.6	64
Hornblende rhyodacite porphyry (includes McDonald and Granite Basin stocks)							40	2.6	134
Christmas intrusive complex	9	3.7	4						
Globe-Miami									
Schultze Granite 'main phase'				7		30			
'Porphyry phase' (Copper Cities, Diamond H)	7		3						
Sierrita									
Ruby Star quartz monzonite porphyry	4.7		1						
Tombstone									
Schieffelin granodiorite							16.2	4	55
Bingham									
Last Chance stock				7.4		10.9			
Monzonite and quartz monzonite				6		6.6			
Quartz monzonite porphyry	16								
Alta									
Equigranular phase				10	2.7	3.7			
Porphyritic phase	5	2.7	7.2						
Brenda									
Quartz diorite and granodiorite	2	2	4						
Ely									
Granodiorite porphyry (Lane Valley sill)							13	4	134
Weary Flat quartz monzonite					2.3	3			
Koloula, Guadalcanal									
Mineralizing intrusions	23	7	22						
Less-mineralizing intrusions (southern part of Inamumu Zoned Pluton)				42	8	29			
Barren tonalite intrusions (2 Ma older than mineralization)								14	380
Barren tonalite intrusions (0.4 Ma younger than mineralization)							600	17	57

with Koloula, an island-arc deposit, magnetite and not biotite is the major Cu-bearing phase in continental North American deposits studied. In both regions magmatic pyroxenes and amphiboles (Table 2 and Hendry et al. 1981) contain insignificant copper, suggesting that possible release of copper during pyroxene hydration to amphibole is unimportant.

In the introduction we outlined processes by which copper is non-incorporated or lost from silicate phases during vapour exsolution. We argued that those components that are strongly partitioned into the vapour phase are depleted in the silicate melt and probably even more so in the crystallizing amphibole and to a lesser extent biotite. The presence of Si- and Mg-rich amphibole domains, commonly ranging in composition from magnesio-hornblende through to actinolite within single grains, in the Christmas intrusive complex, the Alta stock, Weary Flat quartz monzonite at Ely, and in the Brenda composite stock is indicative of element partitioning during vapour exsolution. The high Mg-contents of all magmatic biotites at Bingham, including those from the equigranular Last Chance stock are consistent with vapour exsolution for all pre-mineralization intrusions. Similar X_{mg} values for biotites in the main phase of the Schultze Granite and in nearby Cu-bearing porphyries, that have aphanitic textures related to H_2O-venting (Creasey 1980), suggest that vapour exsolution also occurred in the main phase of the Schultze Granite. We therefore contend that Cu-bearing porphyries and some, if not all, barren type A intrusions have undergone vapour exsolution, during which Cu was lost or abstracted from mafic minerals to produce Cu-depleted minerals reported in this study.

Vapour exsolution does not appear to have occurred in barren type B intrusions. These magmatic amphiboles are more Fe-rich and Si-poor than in mineralized porphyries, and amphiboles in individual barren type B intrusions show only limited compositional variation. Copper is retained in magnetite and to a lesser extent in biotite (Table 3).

The low copper content of mafic minerals from mineralizing and barren type A intrusions reinforces a suspected genetic link suggested by Westra (1979), based on field relations. We strongly support his model that copper is abstracted or partitioned from not only the narrow cylindrical porphyries themselves but also from the deeper level coarse-grained progenitors. The extent to which copper has been removed from these coarse-grained progenitors is evident from sampling of the Last Chance Stock and associated monzonite and quartz monzonite at Bingham (Fig. 7). Biotites and magnetites are Cu-depleted in all samples collected over the outcrop area of these intrusions.

There is thus ample scope for the generation of copper ore bodies by abstraction of perhaps a few tens of ppm Cu from pluton volumes of typically greater than 100 km^3, which is equivalent to a cube with a side of 4.65 km. In the following calculation we assume barren type B stocks are a measure of the initial composition of all stocks in a given region prior to the exsolution of magmatic fluids, despite differences in age and geological setting. If a mineralizing quartz monzonite composed of 6 weight percent biotite and 1 weight percent magnetite were able to extract 20 ppm Cu from that biotite and 100 ppm Cu from that magnetite a total of only 2 ppm Cu would be liberated from the whole rock. If such a process were to operate in an igneous body with a volume of 100 km^2 sufficient copper could be released to form an orebody of 100 million tons of 0.5% Cu ore. These figures represent minimum values because there are other sources of copper that we have not investigated. Some copper could come from interstitial liquid as suggested by Feiss (1978). Quartz and feldspars examined in the aphanitic groundmass of Cu-bearing porphyries contain negligible Cu. Other sources involve Cu-rich chlorite and vermiculite intergrowths (Rehrig and McKinney 1976; Hendry et al. 1981; and this study) which occur as late magmatic/deuteric alteration products, and abundant disseminated microscopic grains of pyrite and less commonly chalcopyrite.

In the introduction we proposed that mafic minerals growing in a late magmatic/hydrothermal environment in Cu-bearing porphyries might be expected to incorporate some Cu from these fluids. The presence of secondary actinolite, magnetite, chlorite and biotite assemblages, commonly containing $>1,000$ ppm Cu, supports this contention.

Acknowledgements. The majority of samples used in this study were collected while Chivas was a visiting scientist at the U.S. Geological Survey, Menlo Park. ARC gratefully acknowledges assistance in the field from Cy Creasey (Globe-Miami); Jaren Swensen (Utah Mines Division, Kennecott, Bingham Canyon); Bill Wilson (Kennecott, Ely); Doug Whitford (Brenda); and Richard West and Dan Aiken (Duval Corporation, Sierrita). We are especially grateful to Randy Koski for providing the samples from Christmas. Samples from the Last Chance stock (Bingham) were collected by DAFH with assistance from Jaren Swensen and Gerry North. Bill Kemp provided samples from the Alta stock.

ARC acknowledges the assistance of Nick Ware during electron microprobe analysis at the Australian National University and Phill Berrie for computing. Steve O'Gallagher provided computing assistance at the University of Sydney and help given by Miss S Binns and Len Hay in the preparation of this paper is much appreciated. Miss DK Benson of the Electron Microscope Unit in the University of Sydney provided technical assistance in the running of the ETEC electron-probe used to check sample homogeneity within and surrounding ion-probe holes. Advice given by Roger Mason on various aspects of the ion-probe was invaluable as was that of a more general nature by the late Norman Henry. The senior author also wishes to acknowledge receipt of a travel grant from the Australian Research Grant Scheme, No. E 8115430 I. The ion-probe unit at Cambridge is supported by the National Environment Research Council as is the Cambridge electron-probe, used to analyse biotites in eight of the samples studied.

References

Al-Hashimi ARK, Brownlow AH (1970) Copper content of biotites from the Boulder Batholith, Montana. Econ Geol 65:985–992

Bray RE, Wilson JE, eds (1975) Guide book to the Bingham mining district. Soc Econ Geol. Bingham Canyon, Utah, Kennecott Copper Corp, 156 p, 2 plates

Candela PA, Holland HD (1984) The partitioning of copper and molybdenum between silicate melts and aqueous fluids. Geochim Cosmochim Act 48:373–380

Chivas AR (1976) Magmatic evolution and porphyry copper mineralization of the Koloula Igneous Complex, Guadalcanal. Int Geol Congr 25th, Sydney, 1:48

Chivas AR (1981) Goechemical evidence for magmatic fluids in porphyry copper mineralization. Part I. Mafic silicates from the Koloula Igneous Complex. Contrib Mineral Petrol 78:389–403

Cooper JR (1973) Geologic map of the Twin Buttes Quadrangle, southwest of Tucson, Arizona. US Geol Survey Misc Geol Inv Map I-745

Cranor JI (1974) Petrology and geochemistry of the calc-silicate zone adjacent to the Alta and Clayton Peak stocks near Brighton, Utah. Brigham Young Univ (Provo, Utah), Geol Studies 21:151–176

Creasey SC (1980) Chronology of intrusion and deposition of porphyry copper ores, Globe-Miami District, Arizona. Econ Geol 75:830–844

Crittenden MD Jr, Stuckless JS, Kistler RW, Stern TW (1973) Radiometric dating of intrusive rocks in the Cottonwood area, Utah. J Res US Geol Sur 1:173–178

Czamanske JK, Wones DR (1973) Oxidation during magmatic differentiation, Finnmarka Complex, Oslo area, Norway. Part 2. The mafic silicates. J Petrol 14:349–380

Feiss PG (1978) Magmatic sources of copper in porphyry copper deposits. Econ Geol 73:397–404

Gilluly J (1956) General geology of central Cochise County, Arizona. US Geol Surv Prof Pap 281, 169 p

Graybeal FT (1973) Copper, maganese and zinc in coexisting mafic minerals from Laramide intrusive rocks in Arizona. Econ Geol 68:785–798

Hards N (1976) Distribution of elements between the fluid phase and silicate melt phase of granites and nepheline synenite. In: Biggar GM (ed) Progress in experimental petrology 3:88–91. Nat Environ Res Council, UK

Hendry DAF, Chivas AR, Reed SJB, Long JVP (1981) Geochemical evidence for magmatic fluids in porphyry copper mineralization. II. Ion-probe analysis of Cu contents of mafic minerals, Koloula Igneous Complex. Contrib Mineral Petrol 78:404–412

Holland HD (1972) Granites, solutions, and base metal deposits. Econ Geol 67:281–301

Kesler SE, Issigonis MJ, Brownlow AH, Damon PE, Moore WJ, Northcote KE, Preto VA (1975) Geochemistry of biotites from mineralized and barren intrusive systems. Econ Geol 70:559–567

Kilinc IA, Burnham CW (1972) Partitioning of chloride between a silicate melt and coexisting aqueous phase from 2 to 8 kilobars. Econ Geol 67:231–235

Koski RA, Cook DS (1982) Geology of the Christmas porphyry copper deposit, Gila County, Arizona. In: Titley SR (ed) Advances in Geology of the Porphyry Copper Deposits Southwestern North America. The University of Arizona Press, Tucson, Arizona, p 353–374

Lanier G, John EC, Swensen AJ, Reid J, Bard CE, Caddey SW, Wilson JC (1978) General geology of the Bingham mine, Bingham Canyon, Utah. Econ Geol 73:1228–1241

Lovering TG (1969) Distribution of minor elements in samples of biotite from igneous rocks. US Geol Surv Prof Pap 650-B:B101–B106

Mason DR (1978) Compositional variations in ferromagnesian minerals from porphyry copper-generating and barren intrusions of the Western Highlands, Papua New Guinea. Econ Geol 73:878–890

McDowell FW, Kulp JL (1967) Age of intrusion and ore deposition in the Robinson mining district of Nevada. Econ Geol 62:905–909

Moore WJ, Czamanske GK (1973) Compositions of biotites from unaltered and altered monzonitic rocks in the Bingham mining district, Utah. Econ Geol 68:269–274

Nash JT, Cunningham CG Jr (1974) Fluid-inclusion studies of the porphyry copper deposit at Bagdad, Arizona. J Res US Geol Surv 2:31–34

Olade MA (1979) Copper and zinc in biotite, magnetite and feldspar from a porphyry copper environment, Highland Valley, British Columbia, Canada. Min Engng 31:1363–1370

Parry WT, Nackowski MP (1963) Copper, lead and zinc in biotites from Basin and Range quartz monzonites. Econ Geol 58:1126–1144

Rehrig WA, McKinney CN (1976) The distribution and origin of anomalous copper in biotite. Soc Mining Engrs AIME preprint 76-L-64, 34 p

Ryabchikov ID (1963) Experimental study of the distribution of alkali elements between immiscible silicate and chloride melts. Dokl Akad Nauk SSSR 149:190–192

Sheppard SMF, Gustafson LB (1976) Oxygen and hydrogen isotopes in the porphyry copper deposit at El Salvador, Chile. Econ Geol 71:1549–1559

Sheppard SMF, Nielsen RL, Taylor HP Jr (1971) Hydrogen and oxygen isotope ratios in minerals from porphyry copper deposits. Econ Geol 66:515–542

Soregaroli AE (1974) Geology of the Brenda copper-molybdenum deposit in British Columbia. Can Min Metall Bull 67 (750):76–83

Soregaroli AE, Whitford DF (1976) Brenda. In: Sutherland Brown A (ed) Porphyry deposits of the Canadian Cordillera. Can Min Metall Special Vol 15:186–194

Steiger RH, Jäger E (1977) Subcommision on geochronology: Convention on the use of decay constants in geo- and cosmochronology. Earth Planet Sci Lett 36:359–362

Warnaars FW, Smith WH, Bray RE, Lanier G, Shafiqullah M (1978) Geochronology of igneous intrusions and porphyry copper mineralization at Bingham, Utah. Econ Geol 73:1242–1249

West RJ, Aiken DM (1982) Geology of the Sierrita-Esperanza deposit, Pima mining district, Pima County, Arizona. In: Titley SR (ed) Advances in Geology of the Porphyry Copper Deposits Southwestern North America. The University of Arizona Press, Tucson, Arizona, p 433–465

Westra G (1979) Porphyry copper genesis at Ely, Nevada. In: Ridge JD (ed) Papers on mineral desposits of western North America. Nevada Bureau Mines Geol Report 33:127–140

Westra G (1982) Alteration and mineralization in the Ruth porphyry copper deposit near Ely, Nevada. Econ Geol 77:950–970

White WH, Harakal JE, Carter NC (1968) Potassium-argon ages of some ore deposits in British Columbia. Can Min Metall Bull 61:1326–1334

Accepted December 6, 1984